Ocean Engineering 160 (2018) 94–104

Contents lists available at ScienceDirect

Ocean Engineering

journal homepage: www.elsevier.com/locate/oceaneng

System reliability of floating offshore wind farms with multiline anchors

Spencer T. Hallowell [a,*], Sanjay R. Arwade [a], Casey M. Fontana [a], Don J. DeGroot [a], Charles P. Aubeny [b], Brian D. Diaz [b], Andrew T. Myers [c], Melissa E. Landon [d]

[a] University of Massachusetts Amherst, USA
[b] Texas A&M University, USA
[c] Northeastern University, USA
[d] University of Maine, USA

ARTICLE INFO

Keywords:
Floating offshore wind
Multiline anchor
Reliability
Progressive failure

ABSTRACT

This research assesses the reliability of floating offshore windfarms utilizing two different anchor configurations: a conventional single-line system in which each anchor is loaded by a single mooring line and a multiline system in which each anchor is loaded by three mooring lines. While there are advantages to adopting a multiline system for floating offshore wind farms, the interconnectedness of this concept introduces disadvantages, such as reduction of system reliability and the potential for cascading failures among multiple structures. The reduction in system reliability is investigated here by running Monte-Carlo simulations in which mooring line and anchor demands and capacities are sampled from probability distributions. Demand distributions are generated through dynamic simulations with environmental conditions corresponding to the 500-year storm. Failure of mooring lines or anchors are initiated when their capacity is exceeded by their demand. The results of this research show that the reliability of the multiline system degrades significantly when progressive failures are taken into consideration. This research also shows that design considerations, such as the sizing of mooring lines and anchors and designing for single-line or multiline loads, significantly influence the system reliability of a floating offshore wind farm.

1. Introduction

As the offshore wind industry continues the trend of installing turbines in deeper water to take advantage of better wind resources (Kumar et al., 2016; Rodrigues et al., 2015), floating offshore wind turbines (FOWTs) are still limited to demonstration projects (Statoil, 2009; Viselli et al., 2016). One of the largest barriers to the development of FOWTs is the increased cost relative to fixed based offshore wind turbines (Myhr et al., 2014). The increased cost of FOWTs can be attributed to additional material costs of larger support structures, increased number of geotechnical investigations needed for multiple anchor locations per turbine, expensive material costs of anchors and mooring lines installed in relatively deeper water than fixed base turbines, and more expensive transmission costs due to longer subsea cables (Myhr et al., 2014). According to the National Renewable Energy Lab (NREL), the substructure and foundation contribute upwards of 35% of the total capital expenditures of a floating offshore wind farm (Moné et al., 2015). To reduce the cost of the anchors of FOWTs, a configuration in which multiple FOWTs share a single anchor is proposed, creating multiline anchors (Diaz et al., 2016). The multiline anchor configuration not only reduces the number of geotechnical investigations and anchors to be fabricated and installed, but also leads to a reduction in the loads on the anchor (Fontana et al., 2016, 2017). One caveat of multiline anchors is that they must be designed for multi-directional loading, which, when combined with certain geotechnical conditions, limits the types of anchors capable of acting as a multiline anchor (Diaz et al., 2016; Fontana et al., 2017).

The introduction of multiline anchors within a FOWT farm means that the failure of an anchor leads to the loss of stationkeeping for multiple turbines. Turbines losing stationkeeping also lead to changes in forces on other interconnected multiline anchors, leading to the potential for cascading failure throughout the farm (Hallowell et al., 2017). For the multiline anchors, the interconnected behavior and potential for cascading effects causes a change in structural reliability for the entire system when compared to conventional single-line anchors (Hallowell et al., 2017). This research extends the authors' previous work by calculating system reliabilities for the floating platforms, rather than component reliabilities, and by comparing systems reliability that results from differing component design methodologies.> For the multiline

* Corresponding author.
E-mail address: shallowell@umass.edu (S.T. Hallowell).

https://doi.org/10.1016/j.oceaneng.2018.04.046
Received 31 October 2017; Received in revised form 26 February 2018; Accepted 15 April 2018

Nomenclature

a_i	anchor number
i	single-line configuration
a_{ijk}	anchor *ijk*, multiline configuration
C_l	line capacity distribution
C_a	anchor capacity distribution
$F_{a,,i}$	anchor tension in anchor i
$F_{l,i}$:	mooring line tension in line i
FOWT	floating offshore wind turbine
l_i	line number i
MRP	mean return period
P_f	probability of failure
SLC	survivability load case
s	coordinate of position along mooring line
s_u	undrained shear strength
t_i	turbine number i
WWC	wind, wave, and current
α	soil adhesion factor
β	reliability index
θ	polar coordinate, counter clockwise from North
θ_{WWC}	wind, wave, and current direction

anchor concept to be implemented in a wind farm, the cascading failure mode must be well understood so that its effects may be incorporated into the overall design of the system. This research investigates the reliability of two components of the proposed multiline anchor system, the anchor and mooring lines, and compares them to their counterparts in a single-line anchor system.

According to Moan, structural damage is a relatively common event, with an occurrence of nearly 18 per 1000 platform-years for floating structures (Moan, 2009). There are several historical examples of failure of mooring lines or anchors of floating offshore structures (Sharples, 2006). For example, during Hurricane Ivan in 2004, the semi-submersible platform Noble Jim Thompson broke multiple mooring lines at the fairlead, leading to progressive failure of other mooring lines and loss of stationkeeping (Sharples, 2006). The loss of stationkeeping produced an out of plane loading on the connections between mooring lines and the padeye of the suction pile anchors, leading to the failure of several padeyes (Sharples, 2006). The Noble Lorris Bouzigard floating platform also experienced mooring failures due to Hurricane Ivan, most notably the failure of mooring lines at the fairleads, leading to anchors being dragged from their original location (Sharples, 2006). The 2005 hurricane season included Hurricanes Katrina and Rita, during which 6 and 13 platforms were set adrift from their moorings, respectively (Cruz and Krausmann, 2008). The most notable failure was that of the semi-submersible Deepwater Nautilus, which broke free from its moorings in Hurricane Ivan in 2004, and then again during Hurricane Katrina due to significant damage of its mooring system (Cruz and Krausmann, 2008; Sharples, 2006). In the above examples, it is assumed that the failure mechanism of the mooring lines and connections were due to ultimate tensile loads on the mooring lines under uni-directional forces.

In the aftermath of Hurricane Ivan, studies of failed mooring systems employing suction caissons for Mobile Offshore Drilling Units (MODUs) by Ward et al. (2008) report out-of-plane angles in excess of 90° in the case of the Deepwater Nautilus and angles approaching 45° in the case of the Noble Jim Thompson. In the latter case, the observed post-storm condition of the 9 anchors in the mooring spread showed the following: four anchors showed no evidence of geotechnical failure, three anchors experienced extreme rotation indicative of yield in pure torsion, and two anchors appeared to fail by an axial-lateral failure mechanism (Ward et al., 2008). None of the anchors actually failed in the sense of a complete pullout. However, one may reasonably conclude that 5 of 9 anchors experienced large deformations capable of degrading the soil to its residual state at the soil-caisson interface.

Less experience exists for the failures of anchors resisting multi-directional forces, as required by a multiline system. Experimental investigations have been conducted on suction caissons through centrifuge testing of specimens with multiline loading and have shown that simultaneous orthogonal loading can be treated as a net load on the caisson along the resultant direction (Burns et al., 2014).

There is little guidance in the literature in how to design mooring systems that are susceptible to cascading failure amongst multiple structures. ABS guidelines reference local accidents such as fires, drop loads, or blasts causing chains of cascading events within a solitary structure (American Bureau of Shipping, 2013). Bae et al. assessed the performance of FOWTs whose mooring lines have broken and found that broken lines may result in hundreds of meters of drift due to loss of stationkeeping and a large reduction in mooring line loads, leading to changes in structural reliability (Bae et al., 2017). The lack of guidance for modeling cascading failure amongst structures, and the effect of this failure mode on structural reliability is the motivation behind this research.

This research aims to quantify the reliability of the multiline anchor and mooring line system for a candidate wind farm, and is compared to the reliability of a single-line configuration. Reliability indices, β, are determined by counting the number of failures from Monte-Carlo analyses of a representative wind farm subjected to 500-year storm conditions. Here, β is defined as $\beta = -\Phi(P_f)$, where P_f is the hourly probability of failure given the 500-year storm, and Φ is the standard normal CDF. Failures are assumed to occur when a random sample from a demand distribution of a mooring line or anchor exceeds a random sample of a capacity distribution. Demand distributions are created from hour-long dynamic time history solutions of a full scale FOWT, including dynamic mooring line action. Capacities of mooring lines and anchors are estimated through four representative design philosophies: realistic single-line, exact single-line, realistic multiline, and exact multiline. Here, a "realistic" design is one which accounts for common design practices, such as accounting for misalignment of mooring lines and anchors during installation, as well as limiting the sizing and dimensions of both anchors and chains to reasonably constructible tolerances. An "exact" design is a theoretical representation of an anchor and mooring system in which the capacity is exactly equal to the demand times the safety factor. For the multiline case, failures are tracked and categorized into four different failure types according to how many mooring lines and anchors fail for a given numerical simulation. Conclusions about the results of the reliability analyses are made, and recommendations about further research are given.

2. Problem statement

The general configuration of the FOWT considered here is shown in Fig. 1, representing a plan view of DeepCwind semisubmersible platform used in this research (Robertson et al., 2014). The DeepCwind semi-submersible is a tri-floater platform that is moored to the seafloor with three mooring lines (l_1, l_2, l_3), each of which is attached to a fairlead at one of the columns and to a pad eye at one of the anchors (a_1, a_2, a_3). A coordinate system is established in which the x coordinate is parallel to l_1 and the x coordinate is perpendicular to l_1. A polar coordinate θ is defined with $\theta = 0°$ in the $+x$ direction and is positive for counterclockwise rotations. The mooring lines are equally spaced with $\theta_1 = 180°$, $\theta_2 = 300°$, $\theta_3 = 60°$.

The focus of this paper is on the reliability of two sets of components of the mooring system: the mooring lines and the anchors, neglecting the fairleads and pad eyes. This reliability depends on the capacity of and demand on the mooring lines and anchors, which are treated here as random processes or variables. Mooring lines and anchors are assumed to be identical so that the mooring line capacities can be represented by C_l and the anchor capacities by C_a.

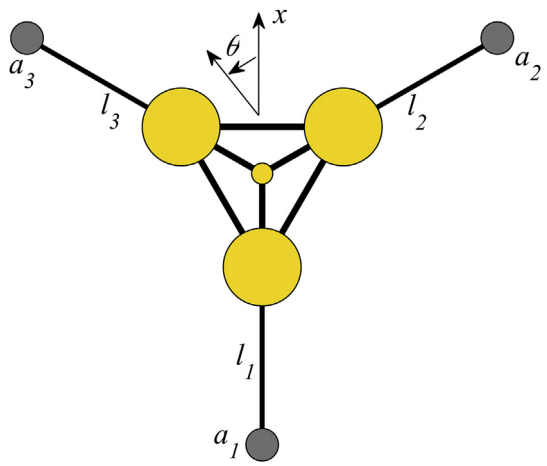

Fig. 1. Plan view of a floating offshore wind turbine configuration using three anchors labelled a_1, a_2, a_3 and three mooring lines labelled l_1, l_2, l_3. Direction θ is measured positive counterclockwise from the x axis. Platform geometry corresponds to a three-hulled semi-submersible with a smaller central column (small yellow circle), to which the turbine tower is attached, between the three pontoons (large yellow circles). (For interpretation of the references to colour in this figure legend, the reader is referred to the Web version of this article.)

Under random dynamic loading from wind, waves, and current (WWC), the FOWT translates and rotates in three dimensions (i.e., six degrees of freedom), generating tension in the mooring lines and forces at the anchor. The tension in mooring line l_i is denoted $F_{l,i}(t,s)$ where the subscript i indicates the line in which the tension occurs, t is time and s is a local curvilinear coordinate defining position along the mooring line, where $s = 0$ is at the fairlead and $s = l_0$ *is* at the pad eye, with l_0 being the length of the mooring lines, which are assumed to be the same length. The mooring line tension changes along the length of the line due to the dynamics of the system and the self-weight of the mooring line. The anchor force $F_{a,i}(t) = F_{l,i}(t,l_0)$ is equal to the mooring line tension at the pad eye.

The maximum values of the anchor and mooring line demands over the time interval $0 < t < t_{\max}$ are $F_{a,i} = \max_{0<t<tmax}(F_{a,i}(t))$ and $F_{l,i}(s) = \max_{0<t<tmax}(F_{l,i}(t,s))$, respectively. Note that the mooring line demand depends on the along-line position s and that the maximum demand at different locations of s may not occur simultaneously. Distributions of the random capacity and demand quantities can be estimated or calibrated from literature, simulation, or theoretical considerations.

The demands and capacities of the three mooring lines l_1, l_2, l_3 are considered mutually independent as are those of the three anchors a_1, a_2, a_3, but, in general, the demands $F_{l,i}(s)$, $i = 1, \ldots,3$ and $F_{a,i}$, $i = 1, \ldots,3$ cannot be treated as identically distributed since the directionality of the loading and motion of the platform results in differing line tensions and anchor forces. The capacities of the mooring lines and anchors are treated here as identically distributed.

Therefore, the failure probability for the single FOWT described above is

$$P_f = 1 - \prod_{i=1}^{3}(1 - P_{fl,i}) \prod_{i=1}^{3}(1 - P_{fa,i}) \tag{1}$$

where $P_{fl,i}$ is the ith mooring line failure probability and $P_{fa,i}$ is the ith anchor failure probability. The anchor failure probabilities $P_{fa,i}$ are straightforward to calculate given the distributions of C_a and $F_{a,i}$ as

$$P_{fa,i} = \mathrm{P}(C_a < F_{a,i}) \tag{2}$$

and the mooring line failure probabilities require comparison of capacity and demand along the entire length of the line, resulting in

$$P_{fl,i} = P(C_l < max_s(F_{l,i}(s))) \tag{3}$$

In practice, Eq. (3) is usually approximated as a summation over a number n_l of links or other finite lengths (Δs) of the mooring chain. The finite lengths correspond to coupons tested experimentally to establish the distribution of the mooring line capacity. Therefore, the failure probability of the line is

$$P_{fl,i} = 1 - \prod_{k=1}^{n_l}(1 - P(C_l < F_{l,i}(s_k))) \tag{4}$$

where $s_k = (k\text{-}1)\Delta s$ defines the positions of the finite lengths of mooring line for which failure is checked.

The multiline anchor system for the use of FOWT stationkeeping requires a new set of indices for the mooring lines and anchors. Here, mooring line l_{ij} is defined as the jth mooring line connected to turbine i. The anchor a_{ijk} refers to the anchor connected to turbines t_i, t_j, and t_k as shown in Fig. 2.

Failure probabilities of mooring lines, anchors, and FOWTs can be calculated for the single line case with some important modifications. Consider the example of Fig. 2 in the case where line l_{k1} has failed. Due to the failure of l_{k1}, the demands on lines l_{k2} and l_{k3} as well as anchor a_{ijk} change. Changes in line and anchor demands necessarily cause changes in anchor failure probabilities. Consider also the case in which turbine t_i is removed from the wind farm, perhaps for servicing. Removal of turbine t_i causes line tensions to become $l_{ij} = 0$, which again alters the demand on anchor a_{ijk}, as well as the other anchors connected to turbine t_i. Also consider the case where line l_{i1} in Fig. 2 fails. This causes the turbine to displace to a new equilibrium position with changing tension demands in lines l_{i2} and l_{i3} and the direction of action of t_i changing significantly relative to its initial direction. Although anchors are indicated as points in the diagrams, the radial distance between the anchor caisson centerline and the pad eye generates a torsion on the caisson when the direction of action of t_i changes. Suction caissons have been demonstrated to lose capacity under torsional effects (Taiebat and Carter, 2005); therefore, both the capacity and demand distribution of a_{ijk} change. Finally, if an anchor itself fails, e.g. a_{ijk} in Fig. 2, each of turbines t_i, t_j, and t_k experience altered dynamics, and each of the lines and anchors connected to said turbines will experience changes in demand. A demonstration of changing multiline anchor demands is given in Fig. 3 for four cases: all lines intact and individual failure of each of the three connected lines. The slight difference between the two failures of downwind lines (blue and yellow) is due to asymmetry in the aerodynamics of the turbine rotor.

3. Multiline system reliability

As described in Section 2, a single FOWT mooring system is

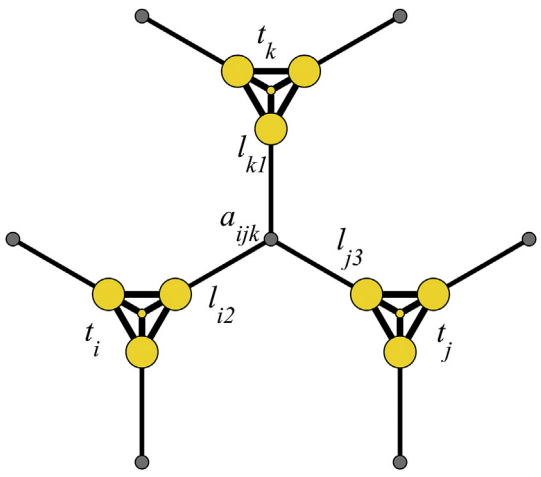

Fig. 2. Plan view of a multiline anchor configuration showing three FOWTs labelled t_i, t_j, t_k connected to the shared anchor a_{ijk}.

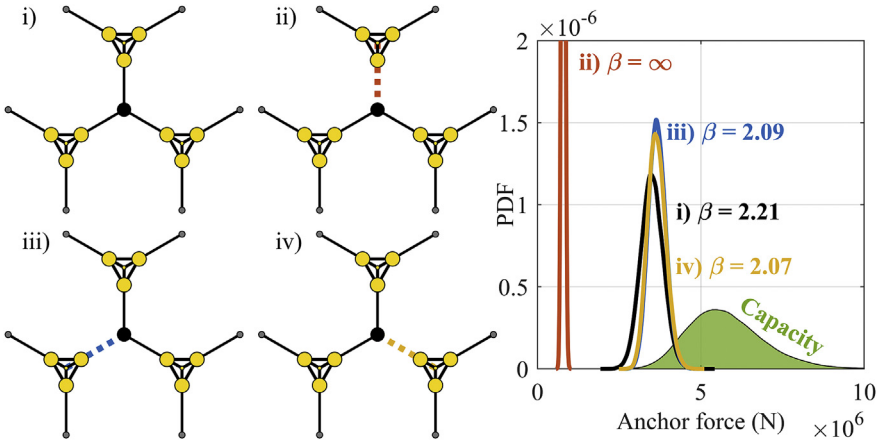

Fig. 3. Changes in multiline anchor demand distributions for individual line failures and $\theta_{WWC} = 0°$.

considered to have failed when at least one of the three mooring lines or one of the three anchors experiences a demand in excess of its capacity. For the interconnected multiline mooring system of an entire FOWT farm, a definition of the system reliability is needed since, by interconnecting the FOWT mooring systems through shared anchors, the individual FOWTs can no longer be treated as distinct engineered systems.

Each mooring system providing stationkeeping for turbine t_i still consists of three mooring lines l_{i1}, l_{i2}, l_{i3} and three anchors a_{ijk}, a_{lim}, *and* a_{noi} where the subscripts *j-o* define the 6 other turbines that are connected to turbine t_i's anchors. Subscript *i* indicates the turbine to the bottom left of the anchor, subscript *j* indicates the turbine to the bottom right of the anchor, and subscript *k* indicates the turbine to the top of the anchor, as shown in Fig. 2.

Given this interconnectedness of the FOWT wind farm system, four different failure modes are defined. In the first three modes the failures are caused by excess demand on mooring components in the undamaged configuration with all mooring lines and anchors intact. In the last mode an initial failure of a mooring line or anchor causes a change in system dynamics and demands on the remaining mooring lines and anchors. In some cases, these demands are larger than in the undamaged configuration meaning that a component that was not overloaded in the undamaged configuration of an FOWT wind farm may become overloaded and fail. Such modes are termed progressive, and, due to the dynamics of the FOWTs, progression occurs in the direction of WWC loading, θ_{WWC}.

1. **Solitary line failure:** At least one mooring line l_{ij}, $j = 1, 2, 3$ connected to FOWT t_i fails and no other components in the system fail. This condition leads to loss of stationkeeping and potential damage for the single FOWT t_i.>
2. **Solitary anchor failure:** A single anchor a_{ijk} fails affecting three FOWTs, t_i, t_j, t_k.> This condition leads to loss of stationkeeping and potential damage for the three FOWTs t_i, t_j, t_k.>
3. **Multiple solitary failures:** More than one FOWT experiences a line or anchor failure under demands corresponding to fully intact mooring systems throughout the wind farm. This condition leads to loss of stationkeeping and potential damage for at least two turbines, but the multiple failures have not resulted from progressive failure in which reconfiguration of the FOWTs after a failure leads to changes in demand on some lines and anchors and subsequent failure.
4. **Progressive failure:** Changes in system dynamics following solitary or multiple solitary mooring line or anchor failures lead to changes in demands on the remaining components. These changes in demand cause additional components to fail in a progressive manner emanating from FOWT t_i or anchor a_{ijk}. Failure progresses outward (in the direction of wind/wave/current loading) from the initial mooring line or anchor failure and is arrested when the failure front reaches a set of components with sufficient capacity to resist modified demands, or when the failure reaches the edge of the wind farm. This condition leads to loss of stationkeeping and potential damage for at least three turbines.

The failure modes are listed above in increasing order of severity, as measured by the number of FOWTs affected by loss of stationkeeping, and, in the results and analysis section, the system reliability of the wind farm is assessed with respect to each system failure mode.

4. Numerical example

A numerical example of a FOWT wind farm is presented to demonstrate the effect of multiline anchors on system reliability. The geometry of the wind farm consists of multiple rows and columns of FOWTs arranged in a staggered grid, as shown in Fig. 3.

The wind farm utilized in this research is a gridded layout of 100 FOWTs, arranged in a configuration of 10 columns and 10 rows with the same orientation as the examples in Fig. 4 and a water depth of 200 m.

The OC4 –DeepCwind semisubmersible platform (OC4 semi-sub) is used in this paper as the representative FOWT design (Robertson et al., 2014). The OC4 semi-sub is based largely on the DeepCwind scaled test floater (Robertson et al., 2013) and consists of a ballast supported tri-floater with three large cylindrical columns acting as pontoons which are connected to a central main column that supports the tower and rotor nacelle assembly (Robertson et al., 2014), as shown in Fig. 5.

The turbine used in this research is the open source NREL 5 MW reference turbine, whose properties are given in Table 1 (Jonkman et al., 2009).

Stationkeeping of the OC4 semi-sub is obtained from three catenary mooring chains extending to the seabed where they are attached to anchors. In this research, suction caissons are used as the representative anchors due to their ability to withstand the multidirectional forces needed in a multiline system. Fig. 2 shows a schematic of the multiline anchor system.

Assessment of the reliability of the FOWT mooring lines and anchors requires reasonable structural properties and therefore designs of the components. The design of the mooring line and anchor system must satisfy criteria for the survival load case (SLC), having prescribed environmental conditions and safety factors for use in the allowable stress design (ASD) design method (5–2 Table 1 for definition of load cases and 8–3 Table 1 for safety factors in *ABS: Guide for Building and Classing Floating Offshore Wind Turbine Installations*) (American Bureau of Shipping, 2015). The mean return period of the environmental conditions and the associated numerical values for the site considered in this paper, along with the prescribed safety factor, are given in Table 2 (Viselli et al., 2014).

This research uses dynamic time history simulations to calculate the

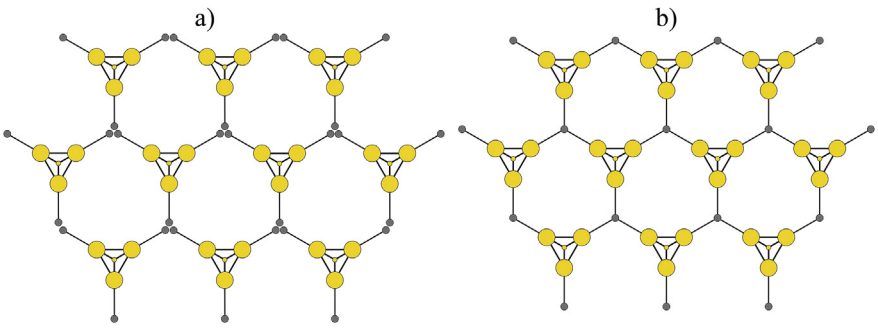

Fig. 4. Example wind farm layout for the single line (a) and multiline (b) configurations. For this example of 10 FOWTs, the number of anchors is reduced from 30 for the single line case to 16 for the multiline case.

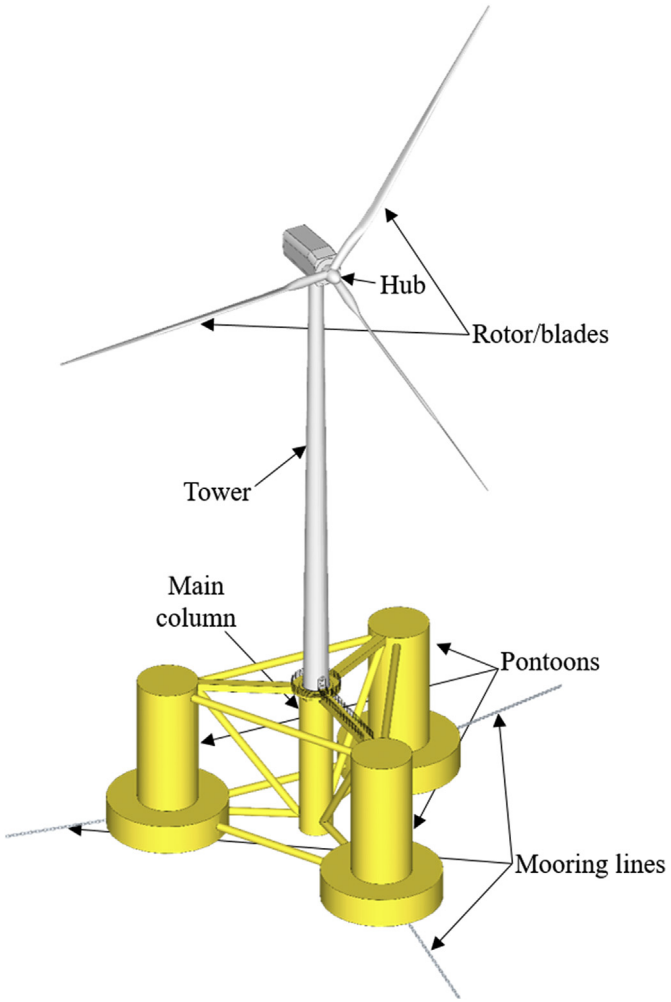

Fig. 5. Schematic of OC4 semi-sub showing three-hulled platform, three mooring lines, tower and rotor nacelle assembly.

nominal demands on the mooring lines. The nominal demand is taken here as the un-factored demand. The simulations are conducted using the open source program FAST, including the effect of turbulent wind following a Kaimal spectrum, irregular waves following a JONSWAP spectrum, structural elasticity, platform rigid body dynamics, and mooring line dynamics modeled with the MoorDyn subroutine (Hall and Goupee, 2015; Jonkman, 2010). The SLC simulations are conducted with the turbine rotor parked and the blades fully feathered, with environmental conditions corresponding to a storm with a 500-year return period. *Forces along the mooring line are sampled at six locations along the length of each line, and at the anchor. Lognormal distributions are fit to the sampled loads and used as the demand distributions to be sampled from in the Monte Carlo simulation.* A detailed description of how the loads obtained from the FAST simulations are used in the design of the mooring lines and suction caisson anchors is given in the following two sections.

Table 1
Properties of the NREL 5 MW turbine.

Rating	5 MW
Rotor Orientation, Configuration	Upwind, 3 Blades
Rotor diameter	126 m
Hub Height	90 m
Cut-In, Rated, Cut-Out Wind Speed	3 m/s, 11.4 m/s, 25 m/s
Rotor Mass	110,000 kg
Nacelle Mass	240,000 kg
Water depth	200 m
Mooring line length	835 m

Table 2
Design environmental conditions and safety factor.

	Mean wind speed		Significant wave height				
	MRP (years)	Design value (m/s)	MRP (years)	Design value (m)	Current (ms^{-1})	Safety Factor	Water Depth (m)
SLC	500	45	500	12.0	0.55	1.05	200

5. Mooring line design

The distributions of the mooring line capacities depend on the design (chain diameter and steel grade) of the mooring system. The design philosophy used for the mooring lines follows the allowable stress design (ASD) methodology given in ABS recommendations for the design of stationkeeping systems for FOWTs (American Bureau of Shipping, 2015). ABS distinguishes between redundant and non-redundant stationkeeping systems and the OC4 semi-sub and its associated 3-line mooring system is considered non-redundant in that the failure of one of the mooring lines leads to the loss of stationkeeping capabilities of the structure (American Bureau of Shipping, 2015). While the OC4 semi-sub has three mooring lines and the FOWT will remain moored in the case of single line failure, the resulting translational offset of the platform would almost certainly damage the electrical connectivity of the turbine. The load effect of interest for the mooring lines is the maximum mooring line tension, taken as the average of the maximum line tensions from six one-hour simulations.

The design requirements are satisfied if the ratio of the nominal capacity to the nominal demand is greater than the prescribed safety factor. Again, the use of nominal implies that no load or resistance factors have been applied. This research estimates mooring line capacity using the

nominal break load capacity of a steel chain segment

$$C_{l,a} = C_g d^2(44 - 0.08d) \quad (5)$$

where $C_{l,a}$ is the nominal break load, C_g is a coefficient corresponding to the grade of steel used, and d is the nominal diameter of the chain (Det Norske Veritas (DNV) 2015).

Two design philosophies are investigated in this research. The first is an "exact" design approach, which sets the capacity of a component exactly equal to the demand times the required safety factor. The second is a "realistic" design approach in which reasonable dimensions and knockdown factors are included in the design of each component. The exact approach allows the intended reliability of the design codes to be assessed, while the realistic approach provides a reliability assessment of as built components, including the effect that over-designed components have on system reliability.

The single-line demands associated with the SLC load case are given in Table 3 below. Grade R3 chain with a nominal diameter of 77.9 mm provides a nominal break load capacity of 5111 kN (Eq. (5)), satisfying the realistic design requirements for the SLC load case. The mean of the lognormal capacity distribution is assumed to be 25% greater than the nominal capacity. A typical design of a FOWT would require checking dozens of other design load cases (DLCs). In the situation where a DLC other than the SLC controls the design, the system reliability will increase for the SLC case. For simplicity, it is assumed here that the SLC case is the controlling design case for the OC4 semi-sub mooring system. This assumption allows the reliability to be calculated for the SLC conditions allowing direct comparison of the multiline configuration to the single-line configuration. The distribution of mooring line capacities is assumed to follow a lognormal distribution with mean equal to 125% of the break load, and a COV of 10% (Choi, 2007). According to Choi (2007), the mean breaking strength of a chain is 25% greater than the reported nominal chain capacity (Choi, 2007).>

6. Anchor design

A suction caisson is designed to resist mooring line loads generated by FOWT dynamic response to WWC loading, and the capacity of this caisson and an associated coefficient of variation define the distribution of the anchor capacity.

Mooring line tensions obtained from the FOWT simulation must be modified before they can be treated as demands on the anchor. The FOWT simulation assumes that anchors act as fixed points at the seabed, whereas the actual attachment point of the mooring line to the anchor (the padeye) is below the seabed, resulting in a reverse catenary profile of the mooring line below the seabed. This reverse catenary causes demand on the anchor to have a vertical component and reduces the resultant tension from that present at the seafloor due to friction between the mooring line and the soil. Here, the padeye is assumed to be at 2/3 of the caisson embedment depth and the method of Neubecker and Randolph is used to determine the reverse catenary geometry and reduction in tension due to friction (Neubecker and Randolph, 1995).

The soil profile used as an example in this paper comprises two units, both soft clays, as described in Table 4.

A key parameter affecting suction caisson anchor capacity is the adhesion factor $\alpha = a/s_u$, where a is adhesion at the soil-caisson interface and s_u is the soil undrained shear strength. The α-factor is most reliably determined from load tests in the field. Extensive databases have been analyzed for piles in (Randolph and Murphy, 1985), which show that α for driven piles can approach unity in normally consolidated clays and decline to less than 0.4 in over-consolidated clays (Randolph and Murphy, 1985). Limited measurements for suction caissons in normally consolidated clays indicate α-values that are somewhat lower than those measured for driven piles, with Jeanjean showing values mostly between $\alpha = 0.65$–0.9 (Jeanjean, 2006). Since a major component of the total axial load capacity of a caisson derives from skin friction (say > 75%), the adhesion factor clearly has a major influence on axial load capacity estimates (Jeanjean, 2006). For laterally loaded anchors for catenary mooring systems, the effect is less pronounced. For the purposes of this example, an adhesion factor of 0.7 is assumed. Over the range of α-factors generally observed, lateral capacity is expected to vary by approximately 5–10%.

Once the vertical and horizontal components of the mooring line tension at the padeye are obtained the caisson capacity is computed based on the outside diameter, embedment depth, and soil properties following the method of Murff and Hamilton (1993), Aubeny (Aubeny et al., 2003), and Aubeny and Murff (2005), which is based on upper bound plasticity methods and accounts for inclined loading.

The primary ultimate capacity calculation assumes that the padeye is located exactly in the plane of the mooring line and that the caisson is perfectly vertical. In actuality, calculated load capacity must usually be adjusted downward due to deviations from this ideal. Twisting of the caisson due to installation misalignment and platform motions place a torsional load on the caisson, which will reduce the available capacity to resist horizontal and vertical loads. Allowances for twist misalignment are typically on the order of 5° due to installation misalignment and 2.5° due to platform motions. The reduction in load capacity due to twist (torsion load demand) varies according to the specifics of a given anchor; however, finite element studies by Cao et al. show a range of load capacity reduction of 2–5% for extreme (hurricane) wind loading and 3–8% for sustained loading (Cao et al., 2005). Generally, the magnitude of capacity reduction due to torsion is less than 5%. In regard to the effects of tilt, a typical installation tilt tolerance is 5°, which changes the relative angle between the anchor and the chain by the same amount. An increased load angle typically decreases anchor capacity, so the possibility of an adverse tilt orientation needs to be considered in the load capacity assessment. In catenary mooring systems, a 5° increase in the load angle is not sufficiently large for load capacity reduction due to interaction effects to be significant, but it can cause significant anchor capacity reductions in taut and semi-taut systems. In designs executed for this paper, a capacity reduction of 5% is included to account for vertical and horizontal misalignment.

The above discussion of twist misalignment is in the context of an intact mooring system. In the event of failure of one or more mooring lines, the loss of station can result in much greater out-of-plane load angles (some reported cases exceed 90°) acting on the caisson (Ward et al., 2008). Based on these experiences in the report by Ward et al. (2008), the present study assumes that, in the event that torsional forces are applied to the caissons, their load capacity will be degraded due to the reduction in soil-caisson adhesion to it residual value.

Anchor pull-out under combined loading is always a possibility, but a more likely scenario is torsional failure, where the anchor spins into the direction of the mooring line. This restores the loading to an in-plane orientation, but the large shear strains at the caisson-soil interface will degrade the soil strength at the soil-caisson interface to a value approaching the remolded strength. In this case the appropriate adhesion factor will be approximately equal to the inverse of the soil sensitivity, with a typical expected range $\alpha = 0.2$–0.4. The effect of this loss of

Table 3
Design demands and capacities for the mooring line used in the numerical example.

	Nominal fairlead demand (kN)	Prescribed safety factor	Nominal capacity (kN)	Mean capacity (kN)	COV of capacity
SLC, realistic design	4016	1.05	5111	6389	10%
SLC, exact design	4016	1.05	4217	5271	10%

Table 4
Soil profile used in caisson design.

Depth (m)	Soil type	Water content (%)	Unit weight (kN/m^3)	Strength at top of layer (kPa)	Linear strength increase rate (kPa/m)	Over-consolidation ratio	Sensitivity
<5	Holocene, high plasticity silt	100	14.3	1.4	0.92	1	6
>5	Pleistocene low plasticity clay	40	17.4	6.4	1.61	1	6

Where the sensitivity is the ratio of intact to remolded undrained shear strength.

adhesion on horizontal load capacity of the anchor will vary according to site-specific conditions, but can be expected to be on the order of 10–20%. In simulations described here, a 20% reduction in caisson capacity is assumed for caissons that experience large torsional loads due to line failures and large platform motions.

The capacity prediction method used here is approximate and intended for use in design with a key simplification that only linear variation of soil properties is permitted. Therefore, the two-layer soil profile described above is represented by an equivalent single layer with a single layer profile with linearly varying strength. The strength at mudline and linear increase rate are chosen so that the linearized soil profile generates the same horizontal (shear) and moment resistance to caisson movement as would be generated by the layered profile. Because the moment and shear forces depend on caisson dimensions, a different linearized, equivalent soil profile must be generated for each candidate caisson design. Nevertheless, this procedure is rapid and efficient and leads to realistic and safe predictions of caisson capacity.

A safety factor of 1.5 is applied to the padeye demand and the outside diameter and embedment depth of the caisson are selected such that an adequate safety factor is provided with as little excess capacity as practicable (American Bureau of Shipping, 2015). Caisson diameters were assumed to be specified in increments of 0.10 m and embedment depth in increments of 0.5 m.

A final design check for installability is required. In this design check, self-weight penetration of the caisson is calculated followed by a comparison of suction (i.e., underpressure) needed to complete installation to suction that would cause plug heave failure. The installation check is completed with a safety factor of 1.5 (American Bureau of Shipping, 2015). The suction capacity required for installation is calculated as sum of the skin friction between soil and the interior and exterior surfaces of the caisson and the bearing capacity along the circumference of the leading edge of the caisson. To complete the installation check, a caisson thickness must also be specified, though this thickness does not affect caisson capacity.

In addition to the calculations for minimum required and maximum allowable underpressure, the installation analysis must also evaluate the reduction in caisson penetration depth due to soil flowing into the interior of the caisson. The amount of heave in the internal plug of soil is usually estimated as some fraction of the volume of soil displaced by the penetrating caisson. Noting that suction installation will draw more soil into the interior of the caisson than jacked or dead weight installation, plug heave calculations normally assumed 50–100% of the displaced soil enters the caisson. The effective length of the caisson to be used in load capacity estimates is taken as the physical length of the caisson minus the predicted plug heave (Andersen et al., 2005).

For the example mooring line tensions shown in Table 3, anchor design loads in Table 5 result.

7. Simulation

A representative 100 FOWT arrangement of ten rows and ten columns is used to evaluate the reliability of the multiline anchor system and compare it to a system with conventional single line anchors. Monte-Carlo simulations are performed to estimate the reliability for the SLC environmental conditions at $\theta_{WWC} = 0$, 30, and 60°. Although θ_{WWC} may vary from 0 to 360°, the rotational symmetry in the platform allows for a reduced set of directions to be investigated. The simulations are initiated by sampling capacities for each of the 300 mooring lines and anchors for the single line anchor configuration and each of the 300 mooring lines and 120 anchors for the multiline anchor configuration. Each of the 835 m long mooring lines is assumed to have six segments, following break load test guidelines for the appropriate chain diameter. For this research, all of the line capacities in the single line anchor and multiline anchor configurations are assumed to follow the same lognormal distribution. The distribution of suction caisson anchor capacities is also assumed to be log-normally distributed, with mean capacity equal to the un-factored capacity given in Table 5 and COV equal to 20% (Choi, 2007). The demands of both the anchors and mooring lines are modeled to be log-normally distributed. The lognormal distributions for demands are derived from the maximum loads calculated from 12 one-hour simulations in FAST. Each hour of simulation utilizes different realizations of the wind and wave conditions. Twelve one-hour simulations are conducted for each of seven possible failure states of a turbine: no lines or anchors failed, l_1, l_2, l_3, l_1l_2, l_2l_3, or l_1l_3 (or their corresponding anchors) failed, and three possible θ_{WWC}: 0, 30 or 60°, resulting in a total of 252 simulations.> The simulations representing failed cases are conducted by running FAST with mooring lines deleted and demand distributions representing the new equilibrium position of the FOWT.> For the undamaged, single-line case, and $\theta_{WWC} = 0°$, the mean demand on the most heavily loaded mooring line is 4016 kN, with a COV of 5.8%, and the mean demand on the most heavily loaded anchor is 3848 kN, with a COV of 5.9% Three configurations of anchor capacities are investigated in this research: a single line anchor system with anchors designed for single line loads, a multiline system with anchors designed for single line loads, and a multiline system with anchors designed for reduced multiline loads. Both the single-line and multiline systems are analyzed for realistic and exact design philosophies.

The simulation progresses by initiating the failure state of all mooring lines and anchors to the null state. Given the null state, demands on lines and anchors are sampled from distributions of extreme loads derived

Table 5
Caisson anchor design parameters. In the 'exact' designs the anchor and mooring lines are assumed to be sized such that the factored demand is precisely matched by the anchor or mooring line capacity. In the 'realistic' designs, anchor and mooring line design variables (caisson diameter, embedment and wall thickness, and mooring line grade and diameter) can vary only in discrete increments resulting in modest overdesign of the components.

		Nominal demand (kN)	Prescribed safety factor	Nominal capacity (kN)	Mean capacity (kN)
Single-line configuration	Realistic design	2565	1.5	3866	3866
	Exact design	2565	1.5	3848	3848
Multiline configuration	Realistic design	2292	1.5	3460	3460
	Exact design	2292	1.5	3848	3848

from the FAST simulations described above. The demands are compared against the capacities, tabulating failures as a component whose demand exceeds its capacity and the state of the components is updated according to the failures. If a component has failed, the demand and capacity distributions for the components connected to the affected turbine are updated.> The demands of the components are then resampled according to the new state, and the simulation continues in this loop until the failure state ceases to change.

8. Results

The results of 100,000 simulations for both the single-line configuration and multiline configuration are summarized in this section. For the single-line configuration, the probability of failure of an anchor is calculated by counting the instances of the demand exceeding capacity, and dividing by the number of simulations.

Fig. 6 represents conditions where certain lines have failed, turbines have been removed from service, or are absent due to multiline anchor configuration at the boundaries of the wind farm. Multiline anchor types are designated by the number of turbines (and associated mooring line) present. For example, a_{ik} has turbines t_i and t_k connected, corresponding to the scheme given in Fig. 2.

In Fig. 7, the blue lines represent the decrease in reliability for a system designed with the same design methodology when using multiline anchors over single line anchors. The red lines in Fig. 7 represent the increase in reliability for the same anchor system when realistic design methods are used over exact design methods.

Monte-Carlo simulations allow estimation of the failure probability of each anchor and line in both the single and multiline configurations. The anchors and lines can then be grouped into anchor subsystems (the set of three anchors mooring a FOWT) and line subsystems (the set of three lines mooring a FOWT). Note that FOWTs at the perimeter of the multiline wind farm will be connected to anchors that have either two or one line attached. Failure probabilities and associated reliability indices for the anchor and mooring line subsystems are directly estimated from simulations for each FOWT in the wind farm, and can then be further combined into a system failure probability and reliability index for each FOWT. Simulation of the multiline wind farm allows for progressive failure of the interconnected mooring system. That is, when a component (anchor or line) fails, the system is reanalyzed in its new configuration and further failures are possible due to changes in demand brought on by the reconfiguration. Results for the multiline wind farm are presented both including and excluding failures that occur in the initial configuration and during failure progression.

Tables 6 and 7 show reliability indices for the anchor and mooring line subsystems for all design cases and WWC directions, including progressive failure. The effect of WWC directionality is clear with the wind farm being far more reliable with respect to $\theta_{WWC} = 60^\circ$ than the worst case $\theta_{WWC} = 0^\circ$. Design of anchors for reduced multiline loading also significantly reduces the reliability, with the lowest reliability index of 0.5 occurring for anchor subsystems designed for multiline loading and subject to $\theta_{WWC} = 0^\circ$. It is important to note that although multiline anchors experience lower demand levels, the demand distribution is equal on all anchors in the wind farm except perimeter anchors, whereas in a single line wind farm only one or two anchors mooring each FOWT are subject to significant loads for any given WWC direction. The lower design capacity and more evenly distributed loading on anchors throughout the wind farm conspire to make reliability for multiline load designed anchors significantly lower than in the single line case.

For both anchors and lines, design using realistic design approaches (5% increase in anchor capacity to account for installation error and the need to specify a chain diameter and strength from a discrete set of choices) leads to a significant increase in reliability that, while it should not be counted upon in a risk assessment, does reflect reserve capacity

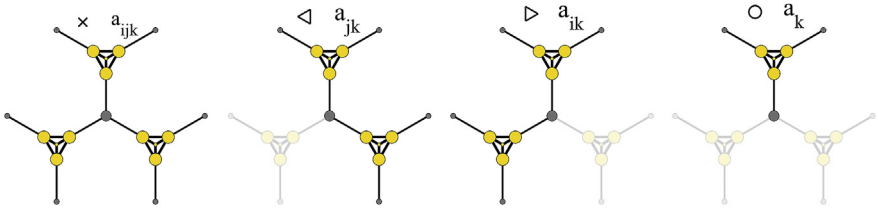

Fig. 6. Multiline anchor configurations with, from left to right, all lines intact, one line failed (two cases) and two lines failed. WWC direction is 0° (upward on the page) meaning that when the heavily loaded line aligned with WWC direction fails anchor reliability approaches infinity. Those cases are therefore omitted. The variability in multiline anchor reliabilities for the $\theta_{WWC} = 0^\circ$ case are shown graphically in Fig. 7 for each of the conditions given in Fig. 6.

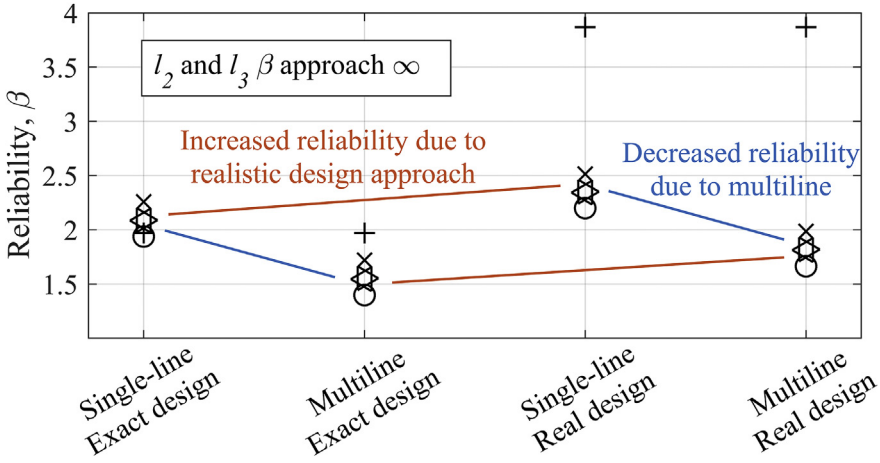

Fig. 7. Variability of anchor and mooring line reliability indices for configurations shown in Fig. 7 and for each of the four design philosophies. Downwind mooring line l_1 reliability also shown with a + marker. Upwind lines l_2 and l_3 are lightly loaded and have reliability that approaches infinity. Symbol markers correspond to those defined in Fig. 6, for the case of $\theta_{WWC} = 0^\circ$.

Table 6
Reliability factors of FOWT anchor subsystems including progressive failures. Results are given for each of the four design philosophies. When the anchor has been designed for reduced forces from multiline loading only results for the case of multiline loading are given. When the anchor has been designed for larger single line forces results are given for the two cases when the anchor is deployed in single or multiline configurations. Reliabilities are lower when anchors are deployed in multiline configurations because of the inclusion of progressive failures in the simulated total count of failed anchors.

WWC direction	Exact, designed for single line force		Exact, designed for multiline force	Realistic, designed for single line force		Realistic, designed for multiline force
	Single -line	Multiline	Multiline	Single-line	Multiline	Multiline
0°	1.9	1.4	0.5	2.2	2.0	1.1
30°	2.6	2.5	1.9	2.9	2.9	2.2
60°	4.2	4.1	3.5	4.4	4.3	3.8

Table 7
Reliability factors of FOWT mooring line subsystems including progressive failures. Reduction of reliability in multiline as opposed to single line cases is due to changes in mooring line forces after anchor failure during progressive failure and associated resampling of mooring line forces from the appropriate distribution.

	Exact, designed for single line force		Exact, designed for multiline force	Realistic, designed for single line force		Realistic, designed for multiline force
	Single-line	Multiline	Multiline	Single -line	Multiline	Multiline
0°	2.0	1.9	1.4	3.9	2.7	2.1
30°	3.3	2.9	2.5	Inf	3.2	2.7
60°	Inf	4.2	3.8	Inf	4.4	4.0

Table 9
Percentage change in mooring line reliability factor when progressive failure is included in the simulation of multiline wind farms. The magnitude of the percentage change, which is always positive, indicates how susceptible the given system and design philosophy is to progressive failure.

	Exact, designed for single line force		Exact, designed for multiline force	Realistic, designed for single line force		Realistic, designed for multiline force
	Single-line	Multiline	Multiline	Single-line	Multiline	Multiline
0°	0%	5%	43%	0%	44%	86%
30°	0%	17%	36%	/	59%	89%
60°	/	/	/	/	/	/

and reliability that is present in many engineered systems.

Tables 8 and 9 give the percent increase in reliability for the same cases as in Tables 6 and 7 but, for multiline wind farms, without the effect of progressive failures. That is, neglecting failures that occur due to reconfiguration of the system after initial component failure. For the single line wind farm, the results in Tables 8 and 9 show no change relative to Tables 6 and 7 and are shown to ease comparison between the single line and multiline cases. For the multiline cases, the reliability indices are significantly higher when progressive failures are excluded. For example, for the exact, single line design with $\theta_{WWC} = 0°$, the reliability index goes from 1.8 to 1.4 when progressive failures are included, representing a 29% change in the reliability index. This illustrates the effect of interconnectedness of the multiline mooring system on overall reliability.

Table 10 lists the rates of occurrence of the four types of failure listed in the System Reliability section for the worst case WWC direction of $\theta_{WWC} = 0°$. For the exact designs, the likelihood of no failure is small because of the large number of FOWTs (100) in the example wind farm, and the probability of progressive failure occurring in a multiline farm is unacceptably high, even when the anchors have been designed for larger single line forces. Realistic designs add significant safety margin and therefore reduce substantially the rates of multiple or progressive failures. Nevertheless, those rates remain greater than what would probably be acceptable to designers and regulators, and therefore methods of mitigating the likelihood of progressive failure in a multiline anchor system should be pursued.

Finally, the simulations performed allow estimation of the reliability of an individual FOWT, as shown in Table 11. Of particular note are the $\theta_{WWC} = 0°$ cases for exact and realistic designs for single line force in a single line wind farm (1st and 4th columns). These reliabilities, 1.7 and 2.2, reflect estimates of the reliability of a FOWT mooring system designed to current code standards.

Table 8
Percentage change in anchor reliability factor when progressive failure is included in the simulation of multiline wind farms. The magnitude of the percentage change, which is always positive, indicates how susceptible the given system and design philosophy is to progressive failure. For example, the most sensitive case is a system designed exactly for reduced multiline loading and loaded in the worst case WWC direction of 0°. In that case more than half the total failures are due to progressive failure (decrease in reliability index of 140%).

	Exact, designed for single line force		Exact, designed for multiline force	Realistic, designed for single line force		Realistic, designed for multiline force
	Single-line	Multiline	Multiline	Single-line	Multiline	Multiline
0°	0%	29%	140%	0%	5%	36%
30°	0%	8%	16%	0%	3%	9%
60°	0%	0%	3%	0%	0%	0%

9. Discussion

The reliability factor of a FOWT designed with a single-line system using the exact design philosophy is 1.7, 2.6, and 4.2 for $\theta_{WWC} = 0°$, 30°, and 60°, respectively. These reliability factors give an indication of what the intended reliability of a FOWT system is when adhering to the different design methodologies outlined in this research. The intended reliabilities decrease for the multiline system when using the exact design philosophy, with reliability factors of 1.3, 2.5, and 4.1 for $\theta_{WWC} = 0°$, 30°, and 60°, respectively. The decrease in multiline reliability is caused by the interconnectedness of the anchor system and the change in demands on the anchor when failures are initiated. The interconnectedness of the multiline anchor system allows for failures to progress from the initiation point, leading to many more component failures than a single-line system with similar capacities. The decrease in multiline anchor reliability persists, even though the initial demand on the anchors in a given simulation is lower, leading to higher initial reliabilities, as shown in Table 6.

There is considerable variability in the reliabilities of mooring lines and anchors within the 100 turbine wind farm, as indicated in Fig. 7. For the multiline system with anchors designed exactly for single line forces, the reliability of l_1 is 1.9 while the reliability of l_3 is 2.8, an order of magnitude difference in the failure probabilities. Anchor reliabilities have similar variability, especially since not all of the anchors within the 100 turbine farm have the same number of lines connected. For the multiline system with anchors designed realistically for multiline forces,

Table 10
Rate of occurrence of the four different failure modes in increasing order of severity.

	Exact, designed for single line force		Exact, designed for multiline force	Realistic, designed for single line force		Realistic, designed for multiline force
	Single line	Multiline	Multiline	Single line	Multi line	Multiline
No failures	0.5%	2.1%	0.1%	25.0%	48.5%	5.5%
Solitary line	1.8%	3.9%	0.1%	0.0%	0.2%	0.0%
Solitary anchor	1.4%	0.0%	0.0%	34.1%	0.0%	0.0%
Multiple solitary	96.0%	29.0%	2.9%	40.8%	35.0%	21.5%
Progressive	NA	65.0%	97.0%	NA	16.2%	NA

Table 11
Individual FOWT reliabilities. These reliability indices β should be taken to reflect the reliability index of the mooring system of a FOWT designed according to current specifications and practices including safety factors. Padeye and fairlead connection failures are neglected in this calculation.

	Exact, designed for single line force		Exact, designed for multiline force	Realistic, designed for single line force		Realistic, designed for multiline force
	Single line	Multiline	Multiline	Single line	Multi line	Multiline
0	1.7	1.3	0.5	2.2	2.0	1.1
30	2.6	2.5	1.9	2.9	2.9	2.2
60	4.2	4.1	3.5	4.5	4.3	3.8

anchor type a_i, or an anchor with only one turbine connected downwind, has the highest reliability index of 1.7, while anchor type a_{ik}, or an anchor with one upwind and one downwind turbine connected, has the lowest reliability index of 1.6.

Designing the anchors for reduced multiline forces reduces the FOWT reliability significantly. For the realistic design philosophy, the reliability index of the multiline FOWT system decreases from 2.0 to 1.1 for designs utilizing single-line and multiline anchor forces, respectively. Thus, incorporating such a reduction should be done with caution and further study. Inclusion of typical design factors such as the 5% knockdown factor for installation misalignment, as well as non-continuous values for anchor and chain dimensions due to construction tolerances, increases the reliability of the FOWTs in both the single-line and multiline systems up to a β of nearly 2.0 for the worst case wind and wave direction of 0° and when designing anchors for single-line forces.

Directionality of the incoming environmental conditions plays an important role in the reliability of the system, with the $\theta_{WWC} = 0°$ case clearly the worst case in terms of anchor and mooring line failures. Angles of environmental conditions away from $\theta_{WWC} = 0°$ cause mooring line tensions and anchor forces to decrease, thereby leading to higher overall system reliabilities. Layouts of FOWT wind farms and their mooring systems are oriented to satisfy both fatigue and ultimate limit state requirements. Therefore, the orientation of a FOWT to mitigate fatigue loads caused by a prevailing WWC direction may not be the optimal orientation to increase reliability in extreme WWC conditions. This study did not take into consideration misalignment between WWC. Inclusion of misalignment would likely increase reliabilities of both the single line and multiline configurations.

10. Conclusions

The reliability of a novel multiline anchor system for FOWTs has been estimated for extreme load conditions and compared to the conventional single line system. Monte-Carlo simulation was utilized to conduct simulations in which capacities and demands of mooring lines and anchors were sampled from probability distributions. Distributions of capacities were developed for exact and realistic design philosophies for both the single-line and multiline systems through the use of design techniques that replicate what is commonly used in the industry. Distributions of demands were calculated by running dynamic numerical simulations of the OC4 semi-sub for various environmental loading directions. Reliabilities were estimated by conducting 100,000 simulations of a representative 100 turbine wind farm tallying failures when the demand of a mooring line or anchor component exceeds its capacity, and converting to reliabilities using the inverse standard normal CDF. System reliabilities for various design methodologies ranged from $\beta = 0.5$ for a multiline system designed for multiline forces using an exact design methodology, to a reliability of $\beta = 2.2$ for a single-line system using a realistic design methodology for a wind, wave and current direction of0°. Variability of the reliability index of individual mooring lines and anchors ranges from $\beta = 1.4$ for multiline anchors connected to three turbines in a system with anchors designed for exact multiline forces, to β nearly infinite for l_3 mooring lines in a system with anchors designed for realistic single-line forces. Progressive failures were a contributing factor in the decrease in multiline system reliabilities when compared to the single-line system, and should be accounted for in the design of multiline FOWT systems.

Acknowledgements

The authors acknowledge funding from the US National Science Foundation through grants CMMI-1463273 and CMMI-1552559 and from the Massachusetts Clean Energy Center.

References

American Bureau of Shipping, 2013. Guidance Notes on Accidental Load Analysis and Design for Offshore Structures. (February).
American Bureau of Shipping, 2015. Guide for building and classing floating offshore wind turbine installations. Standardization.
Andersen, K.H., Murff, J.D., Randolph, M.F., Clukey, E.C., Erbrich, C.T., Jostad, H.P., Hansen, B., Aubeny, C.P., Sharma, P., Supachawarote, C., 2005. Suction anchors for deepwater applications. Frontiers in offshore geotechnics. In: ISFOG 2005-Proceedings of the 1st International Symposium on Frontiers in Offshore Geotechnics, pp. 3–30.
Aubeny, C.P., Han, S., Murff, D.J., 2003. Refined model for inclined load capacity of suction caissons. Pp. 883–87. In: ASME2003 22nd International Conference on Offshore Mechanics and Arctic Engineering.
Aubeny, C.P., Murff, D.J., 2005. Simplified limit solutions for the capacity of suction anchors under undrained conditions. Ocean. Eng. 32 (7 Special Issue), 864–877.
Bae, Y.H., Kim, M.H., Kim, H.C., 2017. Performance changes of a floating offshore wind turbine with broken mooring line. Renew. Energy 101, 364–375 (https://doi.org/10.1016/j.renene.2016.08.044).
Burns, M., Maynard, M.L., Davids, W.G., Chung, J., Gaudin, C., 2014. In: Centrifuge Modelling of Suction Caissons under Orthogonal Double Line Loading. 8th ICPMG, pp. 465–471.
Cao, J., Li, Y., Tjok, K.M., Audibert, J.M.E., 2005. Validation of the use of beam-column method for suction caisson design. In: Frontiers in Offshore Geotechnics, ISFOG 2005-Proceedings of the 1st International Symposium on Frontiers in Offshore Geotechnics (2000), pp. 325–331.
Choi, Y.J., 2007. Reliability Assessment of Foundations for Offshore Mooring Systems under Extreme Environments. The University of Texas at Austin.
Cruz, A.M., Krausmann, E., 2008. Damage to offshore oil and gas facilities following hurricanes Katrina and Rita: an overview. J. Loss Prev. Process Ind. 21 (6), 620–626.
Det Norske Veritas (DNV), 2015. Offshore Standard DNV-OS-E302: Offshore Mooring Chain.
Diaz, B.D., Rasulo, M., Aubeny, C.P., Fontana, C.M., Arwade, S.R., Degroot, D.J., Landon, M.E., 2016. Multiline anchors for floating offshore wind towers. In: OCEANS 2016 MTS/IEEE Monterey, vol. 2016. OCE.
Fontana, C.M., Arwade, S.R., DeGroot, D.J., Hallowell, S.T., Aubeny, C.P., Landon, M.E., Myers, A.T., Hajjar, J.F., Ozmultu, C., 2017. Multiline anchors for the OC4

semisubmersible floating system. In: The 27th International Ocean and Polar Engineering Conference. International Society of Offshore and Polar Engineers.
Fontana, C.M., Arwade, S.R., DeGroot, D.J., Myers, A.T., Landon, M.E., Aubeny, C.P., 2016. Efficient multiline anchor systems for floating offshore wind turbines. In: ASME 2016 35th International Conference on Ocean. Offshore and Arctic Engineering.
Hall, M., Goupee, A., 2015. Validation of a lumped-mass mooring line model with DeepCwind semisubmersible model test data. Ocean. Eng. 104, 590–603.
Hallowell, S.T., Arwade, S.R., Fontana, C.M., DeGroot, D.J., Diaz, B.D., Aubeny, C.P., Landon, M.E., 2017. Reliability of mooring lines and shared anchors of floating offshore wind turbines. In: I. S. of O, P. Engineers (Eds.), The 27th International Ocean and Polar Engineering Conference.
Jeanjean, P., 2006. Setup characteristics of suction anchors for soft gulf of Mexico clays: experience from field installation and retrieval. In: Offshore Technology Conference.
Jonkman, J., 2010. NWTC design codes (FAST). In: NWTC Design Codes.
Jonkman, J., Butterfield, S., Musial, W., Scott, G., 2009. Definition of a 5-MW Reference Wind Turbine for Offshore System Development (No. NREL/TP-500-38060). National Renewable Energy Lab. (NREL), Golden, CO (United States).
Kumar, Y., Ringenberg, J., Depuru, S.S., Devabhaktuni, V.K., Lee, J.W., Nikolaidis, E., Andersen, B., Afjeh, A., 2016. Wind Energy: trends and enabling technologies. Renew. Sustain. Energy Rev. 53, 209–224.
Moan, T., 2009. Development of accidental collapse limit state criteria for offshore structures. Struct. Saf. 31 (2), 124–135 (https://doi.org/10.1016/j.strusafe.2008.06.004).
Moné, C., Hand, M., Bolinger, M., Rand, J., Heimiller, D., Ho, J., 2015. Cost of Wind Energy Review. (March).
Murff, J.D., Hamilton, J.M., 1993. P-ultimate for undrained analysis of laterally loaded piles. J. Geotech. Eng. 119 (1), 91–107.
Myhr, Anders, Bjerkseter, Catho, Ågotnes, Anders, Nygaard, Tor a, 2014. Levelised cost of Energy for offshore floating wind turbines in a life cycle perspective. Renew. Energy 66, 714–728 (https://doi.org/10.1016/j.renene.2014.01.017).
Neubecker, S.R., Randolph, M.F., 1995. Profile and frictional capacity of embedded anchor chains. J. Geotech. Eng 121 (11), 797–803.
Randolph, M.F., Murphy, B.S., 1985. Shaft capacity of driven piles in clay. Offshore Technol. Conf.
Robertson, A., Goupee, A., Jonkman, J., Prowell, I., Molta, P., Coulling, A., Masciola, M., 2013. Summary of conclusions and recommendations drawn from the deepcwind scaled floating offshore wind system test campaign. In: Proceedings of the ASME 2013 32nd International Conference on Ocean, Offshore and Arctic Engineering (July 2013), pp. 1–13.
Robertson, A., Jonkman, J., Masciola, M., 2014. Definition of the Semisubmersible Floating System for Phase II of OC4. Golden, CO (September):38.
Rodrigues, S., Restrepo, C., Kontos, E., Teixeira Pinto, R., Bauer, P., 2015. Trends of offshore wind projects. Renew. Sustain. Energy Rev. 49, 1114–1135 (https://doi.org/10.1016/j.rser.2015.04.092).
Sharples, M., 2006. Post Mortem Failure Assessment of MODUs during Hurricane Ivan, pp. 1–97.
Statoil, 2009. Hywind Demo. 2009. http://www.statoil.com/en/TechnologyInnovation/NewEnergy/RenewablePowerProduction/Offshore/Hywind/Pages/HywindPuttingWindPowerToTheTest.aspx?redirectShortUrl=http%3A%2F%2Fwww.statoil.com%2Fhywind.
Taiebat, H.A., Carter, J.P., 2005. A failure surface for caisson foundations in undrained soils. Frontiers in offshore geotechnics. In: ISFOG 2005-Proceedings of the 1st International Symposium on Frontiers in Offshore Geotechnics, pp. 289–295.
Viselli, A.M., Goupee, A.J., Dagher, H.J., 2014. Model test of a 1:8 scale floating wind turbine offshore in the gulf of Maine. In: ASME 2014 33rd International Conference on Ocean, Offshore and Arctic Engineering 137(August), pp. 1–11.
Viselli, A.M., Goupee, A.J., Dagher, H.J., Allen, C.K., 2016. Design and model confirmation of the intermediate scale VolturnUS floating wind turbine subjected to its extreme design conditions offshore Maine. Wind Energy 19 (6), 1161–1177.
Ward, E.G., Mercier, R.S., Zhang, J., Kim, M.H., Aubeny, C.P., Gilbert, R.B., 2008. No Modus Adrift. Report Prepared for the Minerals Management Service, College Station, Texas.